Last edited by CLD on 2/20/11.

END-LOADED SHALLOW CURVED BEAMS

Clive L. Dym, F. ASCE
Fletcher Jones Professor of Engineering Design
Department of Engineering
Harvey Mudd College
Claremont, CA 91711

ABSTRACT

This note examines the linear response of thin, shallow curved beams to an axially-directed compressive load. The response is tracked with a rise parameter drawn from related work on linear arches, through which it is shown that the curved beam behaves like an axially compressed bar for small values of the rise parameter, while it responds as a beam in bending for large values of the parameter. This is totally opposite to that of laterally loaded arches.

INTRODUCTION

A previous paper (Dym and Williams 2010) showed that the linear response of arch structures to lateral (both gravitational and centrally directed) loading can be tracked via an arch rise parameter, λ, that is a function of the arch's semi-vertex angle α, thickness h, and radius R: when $\lambda^2 << 1$ the structure responds as a beam in bending, while for $\lambda^2 >> 1$ the response is that of a classical arch in pure compression. The model is linear because neither bifurcation nor snap-through buckling are considered: axial and bending responses to the lateral pressure are coupled by the arch's curvature. Further, the arch's supports are held immobile. It is interesting to ask, How would a similar arch-like structure respond when subjected to a compressive axial—rather than lateral—load (Figure 1)? Further, should such a structure be viewed as a curved beam or as a segment of a ring?

Clearly, the major difference is that one of the supports has to be allowed to move. In addition, while there is a geometric resemblance to a curved beam, the loading is not lateral, as is expected in typical beam analysis. There is a sufficiently long history of work on curved beams and rings that such analyses are now routinely covered in structures and advanced strength of materials textbooks

*Accepted for publication in the **Journal of Structural Engineering** (ASCE).*

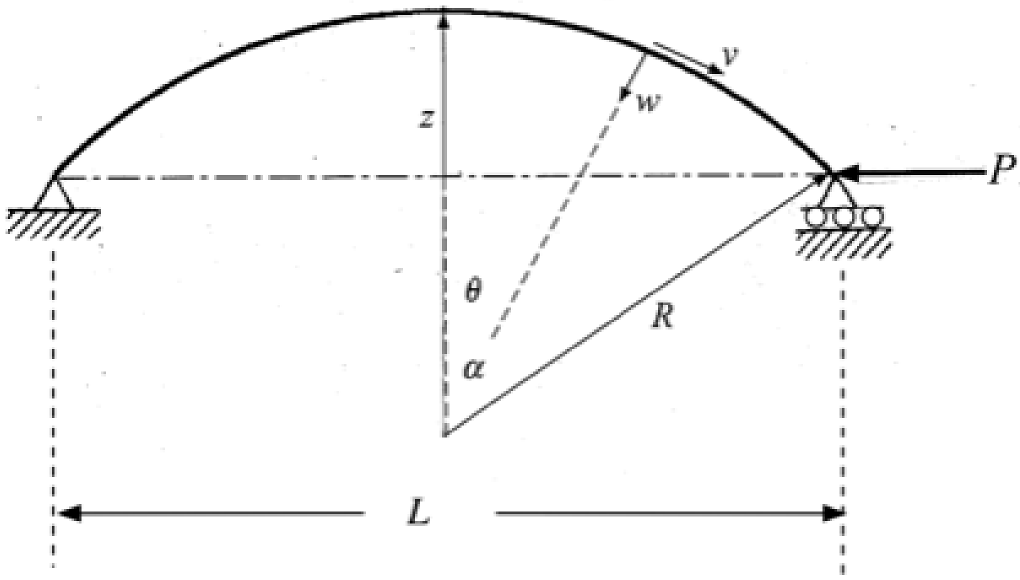

Figure 1. Geometry of and loading on a thin circular (pinned) shallow curved beam of radius *R*, span length *L*, and semi-vertex angle *α*.

(e.g., (Armenàkas 2006; Budynas 1999; Boresi and Schmidt 2003; Hoff 1956). However, virtually all of this work is focused on calculating deflections at discrete points of relatively thick rings, using Castigliano's second theorem. The present work notes the similarity of both the appearance (Figure 1) and the underlying mathematical model of an axially compressed, arch-like structure. Thus, as with a true arch (e.g., (Dym and Williams 2011)), the axial and bending responses are also coupled here, with a purely linear model and once again due to the curvature. This stands in contrast, for example, to the analysis of a straight beam-column, wherein the coupling of axial and bending responses occurs due to a linearized axial load term in the equation of equilibrium. It also stands in contrast to the linearized and nonlinear stability analyses of thin arches (Dym 2002). Thus, it will be shown below that the behavior of such curved beams or arch-like structures under axial loading is precisely the opposite of that exhibited by the true arch: the structure responds as a straight axially-loaded bar when $\lambda^2 << 1$ and as a beam in bending when $\lambda^2 >> 1$.

SHALLOW CURVED BEAMS UNDER END LOADING

Consider a planar circular curved beam of constant mean radius R and thickness h, loaded at one (moveable) end by a concentrated axial load P (Figure 1). The curved beam is taken as shallow, in which case the curvature change, expressed in terms of tangential and radial displacements, respectively v and w, may be approximated as $\kappa = -(z/R^2)\left(w''(\theta) + v'(\theta)\right) \cong -(z/R^2)\left(w''(\theta)\right)$. Then the first variation of the total potential energy for such an arch-like structure is adapted from (Dym and Williams 2011) as

$$\delta^{(1)}\Pi = \int_{-\alpha}^{\alpha} \left\{ \frac{N}{R}\left[\frac{d\delta v}{d\theta} - \delta w\right] - \frac{M}{R^2}\left(\frac{d^2\delta w}{d\theta^2}\right)\right\} R\,d\theta - P\left(\delta w(\alpha)\sin\alpha - \delta v(\alpha)\cos\alpha\right) \qquad (1)$$

where the constitutive relations for the stress resultants are written in terms of the displacements as

$$\begin{aligned} N(\theta) &= \frac{EA}{R}\left(\frac{dv(\theta)}{d\theta} - w(\theta)\right) \\ M(\theta) &= -\frac{EI}{R^2}\left(\frac{d^2w(\theta)}{d\theta^2}\right) \end{aligned} \qquad (2)$$

Note that Eq. (1) reflects the constraint that the moveable support translates only along the line of the horizontally applied load P, that is, no vertical movement is allowed. The equilibrium equations follow from the customary integration-by-parts and vanishing of Eq. (1) as

$$\begin{aligned} \frac{dN(\theta)}{d\theta} &= 0 \\ N(\theta) + \frac{1}{R}\frac{d^2M(\theta)}{d\theta^2} &= 0 \end{aligned} \qquad (3)$$

The vanishing of Eq. (1) also produces boundary conditions at the ends of the arch, $\theta = \pm\alpha$. For the pinned arch considered here, four of the six required conditions are familiar,

$$v(-\alpha) = 0, \quad w(-\alpha) = 0, \quad M(-\alpha) = 0, \quad M(\alpha) = 0 \qquad (4)$$

A fifth boundary condition states horizontal equilibrium at the loaded tip,

$$\frac{1}{R}\frac{dM(\alpha)}{d\theta}\sin\alpha - N(\alpha)\cos\alpha = P \tag{5}$$

while the sixth reflects constrained horizontal motion at the moveable support,

$$w(\alpha) + v(\alpha)\tan\alpha = 0 \tag{6}$$

The stress resultants satisfying the equilibrium equations (3), the two moment boundary conditions (4), and the first of the constrained boundary conditions (5) are then found to be

$$N(\theta) = -N_0 = -\frac{P}{\cos\alpha(1+\alpha\tan\alpha)} \tag{7}$$

and

$$M(\theta) = \left(N_0 R/2\right)\left(\theta^2 - \alpha^2\right) \tag{8}$$

The corresponding tangential and radial displacements are found by integrating the corresponding constitutive equations (2) under appropriate boundary (4) and constraint (6) conditions. It is convenient when expressing those displacements to introduce an dimensionless rise parameter λ used by Dym and Williams (2011) to track linear arch behavior. It was first defined by Schreyer and Masur (1966) as the (dimensionless) ratio of the arch rise f to one-half of the arch thickness h (see Figure 1):

$$\lambda \triangleq \frac{f}{h/2} = \frac{2R}{h}\left(\frac{f}{R}\right) = \frac{2R}{h}\left(1-\cos\alpha\right) \cong \frac{\alpha^2 R}{h} \tag{9}$$

The rise parameter can also be written in terms of the arch's developed length S and its span length L:

$$\lambda \cong \frac{S^2}{4Rh} \cong \frac{L^2}{4Rh} \tag{10}$$

For the case of rectangular cross-section, the arch rise parameter can be identified with the ratio of the bending stiffness to the extensional stiffness. That is, when $A = bh$ and $I = bh^3/12$, it is easily seen that:

$$\frac{EI/R^3}{EA/R} = \frac{I}{AR^2} \equiv \frac{\alpha^4}{12\lambda^2} \tag{11}$$

With the aid of the definitions (9) and (11) in particular, the tangential and radial displacements can be determined and written as, respectively,

$$v(\theta) = \begin{bmatrix} \lambda^2\left(-\frac{5}{2}\left(\frac{\theta}{\alpha}\right)+\left(\frac{\theta}{\alpha}\right)^3-\frac{1}{10}\left(\frac{\theta}{\alpha}\right)^5-\frac{8}{5}\right)-\left(\frac{\theta}{\alpha}+1\right) \\ +\frac{\alpha\tan\alpha}{2(1+\alpha\tan\alpha)}\left(1+8\lambda^2/5\right)\left(\frac{\theta}{\alpha}+1\right)^2 \end{bmatrix}\left(\frac{N_0 R\alpha}{EA}\right) \tag{12}$$

and

$$w(\theta) = \left[\lambda^2\left(-\frac{5}{2}+3\left(\frac{\theta}{\alpha}\right)^2-\frac{1}{2}\left(\frac{\theta}{\alpha}\right)^4\right)+\left(\frac{\alpha\tan\alpha}{1+\alpha\tan\alpha}\right)\left(1+8\lambda^2/5\right)\left(\frac{\theta}{\alpha}+1\right)\right]\left(\frac{N_0 R}{EA}\right) \tag{13}$$

INTERPRETING CURVED BEAM BEHAVIOR

While the meaning of the foregoing results is not immediately evident, some useful estimates of the response of the arch-like structure to an end load can be obtained under the shallow arch (small values of α) assumption. These displacement and stress estimates are explicit functions of the arch rise parameter λ. To begin with, the axial stress resultant (7) becomes

$$N(\theta) = -N_0 \cong -\frac{P}{1+\alpha^2/2} \cong -P \tag{14}$$

The result (14) and the definition (11) of the rise parameter together enable the evaluation of the moment resultant (8) at the curved beam's midpoint ($\theta = 0$) as:

$$M(0) = -N_0 R\alpha^2/2 \cong -Pf \tag{15}$$

Eq. (15) accurately reflects the moment produced by the (only) external load. Also, the midpoint moment vanishes as the arch rise tends to zero, i.e., as $f \to 0$.

The displacements at the midpoint of this arch-like structure are also interesting. In the tangential or in-plane direction, and assuming small angles,

$$v(0) = -\left(\frac{2+\alpha\tan\alpha}{2(1+\alpha\tan\alpha)}\right)\left(1+8\lambda^2/5\right)\left(\frac{N_0 R\alpha}{EA}\right) \cong -\left(1+8\lambda^2/5\right)\left(\frac{PL}{2EA}\right) \tag{16}$$

Eq. (16) clearly shows that for end-loaded curved beams with very small rises, for which $\lambda^2 << 1$, the tangential displacement tends to the exact result that would be expected at the midpoint of an axially loaded straight bar, that is,

$$v(0)\big|_{\lambda^2<<1} \cong -\left(\frac{PL}{2EA}\right) \tag{17}$$

This is quite unlike the laterally loaded arches of (Dym and Williams 2011) which behaved like beams in the small rise limit. The radial displacement at the midpoint also exhibits similar behavior, that is,

$$w(0)\big|_{\lambda^2<<1} \cong \left(\frac{\alpha\tan\alpha}{1+\alpha\tan\alpha}\right)\left(\frac{N_0 R}{EA}\right) \cong \alpha^2\frac{PR}{EA} \cong \alpha\frac{PL}{2EA} \tag{18}$$

In this small rise limit, the radial displacement is smaller than the in-plane displacement by a factor of α, as would be expected for an axially loaded, nearly straight bar.

It is also interesting in this context to calculate the axial stiffness of an almost-straight, axially loaded bar, which here is:

$$\begin{aligned} k &\triangleq \frac{-P}{v(\alpha)/\cos\alpha} \equiv \frac{P}{w(\alpha)/\sin\alpha} \\ &= \frac{EA}{L}\left(\frac{\cos^2\alpha(1+\alpha\tan\alpha)^2}{1+8\lambda^2/5}\right) \end{aligned} \tag{19}$$

For small values of α, then,

$$k \cong \frac{EA}{L}\left(\frac{1}{1+8\lambda^2/5}\right) \tag{20}$$

Eq. (20) obviously produces a familiar limit as $\lambda^2 \to 0$, and also suggests that a slightly bent bar is less stiff than a straight bar. (It ought to be borne in mind that the loaded tip is not free: it is constrained to move in a horizontal direction.) When $\lambda^2 >> 1$, the axial stiffness gets much smaller, as would be expected for a (curved) beam for which bending—rather than extension—is the primary response.

Beyond that, the general behavior of the end-loaded bar as $\lambda^2 >> 1$ is less clear. The mid-point circumferential displacement (16) becomes

$$v(0)\big|_{\lambda^2>>1} \cong -\frac{8\lambda^2}{5}\left(\frac{N_0\alpha R}{EA}\right) \equiv -\frac{\alpha(Pf)L^2}{15EI} \tag{21}$$

while the midpoint radial displacement (18) tends to

$$w(0)\big|_{\lambda^2>>1} \cong -\frac{5\lambda^2}{2}\left(\frac{N_0 R}{EA}\right) \equiv -\frac{5(Pf)L^2}{48EI} \tag{22}$$

Eqs. (21) and (22) exhibit bending response of a beam to an applied moment proportional to *Pf*: a simply supported beam with a clockwise moment *Pf* at its right end produces a midpoint deflection of $w(0) = -PfL^2/16EI$, which is 60% of the value given by Eq. (22). Eq. (21) also shows that the in-plane displacement at the midpoint is smaller than the transverse displacement by a factor of $(16\alpha/25)$, which would be consistent with expectations for such a bent beam. Further, Eqs. (18) and (22) show that the midpoint deflection changes sign and direction as λ^2 increases. Again for small α, it can be shown that there is a transitional value of the rise parameter, $\lambda^2_{trans} \cong 2\alpha^2/5$, for which the midpoint deflection vanishes, i.e., $w(0) = 0$, with the curved beam deflecting outward for $-\alpha \le \theta < 0$ and inward for $0 < \theta \le \alpha$. Similarly, the value of θ at which that transition occurs varies with both α and λ.

Finally, a transition point from bar-to-beam behavior can be identified by examining the circumferential stress of the arch, that is,

$$\sigma_{\theta\theta}(\theta,z) = \frac{N(\theta)}{A} + \frac{M(\theta)z}{I} \tag{23}$$

Evaluated at the curved beam's midpoint, using the results (7) and (8) and the definitions (9) and (11), Eq. (23) becomes:

$$\sigma_{\theta\theta}(0,-h/2) \cong -\frac{P}{A}[1-3\lambda] \tag{24}$$

Thus, for $\lambda << 1/3$, the stress will be the purely compressive state expected in an arch, while for $\lambda >> 1/3$ the stress changes sign as it reflects bending behavior. This is consistent with the results presented earlier.

CONCLUSIONS

This note explored the linear response of shallow curved beams (or arch-like structures) to an axial end load. It was shown that the curved beam behavior ranges from compression of a straight bar, for very shallow arch-like structures, to a bending state for steep curved beams. This behavior stands in stark contrast to that exhibited by laterally loaded true arches when tracked with the same geometric rise parameter λ. Further, inasmuch as the dependence of axial and bending stresses (as well as displacements) on that rise parameter is reasonably evident, the transition from extensional to bending response is readily identified for that end-loaded curved beam.

ACKNOWLEDGEMENTS

The author gratefully acknowledges continuing conversations with his colleague, Emeritus Professor Harry E. Williams, and the thoughtful (and rapid!) reviews that enhanced the clarity of presentation.

REFERENCES

Armenàkas, A. E. (2006). *Advanced Mechanics of Materials and Applied Elasticity*, CRC Taylor & Francis, Boca Raton, Florida.

Boresi, A. P., and Schmidt, R. J. (2003). *Advanced Mechanics of Materials*, 6th Edition, John Wiley, New York.

Budynas, R. G. (1999). *Advanced Strength and Applied Stress Analysis*, 2nd Edition, McGraw-Hill, New York.

Dym, C. L., and Williams, H. E. (2011). "Stress and Displacement Estimates for Arches," *Journal of Structural Engineering*, *137* (1), pp. xxx-xxx.
Hoff, N. J. (1956). *The Analysis of Structures*, John Wiley, New York.
Schreyer, H. L., and Masur, E. F. (1966). "Buckling of Shallow Arches," *Journal of the Engineering Mechanics Division*, ASCE, *92* (EM4), 1-19.